

## THERMAL ANALYSIS OF CRYOCYCLING

Yoed Rabin<sup>1,\*</sup> and Ben-Zion Maytal<sup>2</sup>

<sup>1</sup>Department of Mechanical Engineering, Technion, Haifa 32000, Israel

<sup>2</sup>Cryogenic Section, Rafael, P.O. Box 2250(39), Haifa 31021, Israel

**Summary:** It has recently been suggested that cryocycling may enhance cryodestruction. The term cryocycling refers to a cooling protocol where the cryoprobe temperature oscillates at relatively high frequency around a particular average cryogenic temperature. The main concept is that the temperature oscillations lead to local freezing/thawing cycles at the freezing front, as the freezing front propagates outwards. The thermal analysis presented here indicates that the frequency of temperature oscillations, caused by the cryoprobe, is conserved throughout the entire frozen region while its amplitude decays with the radius. The analysis further indicates high periodic cooling/warming rates within the phase transition region, which may affect the ice formation regime.

**Keywords:** Cryosurgery, Cryocycling, Multi Cycle, Mathematical Model

### Introduction

It has recently been suggested that high-frequency multicycle cryoprotocols may enhance cryodestruction (5,11). The term multicycle cryoprotocol has been used traditionally to indicate a procedure consisting of two or more consecutive freezing/thawing cycles, where complete thawing indicates the end of a cycle. By contrast, the term multicycle cryoprotocol used here is referring to a cooling protocol where the cryoprobe temperature oscillates around a particular average cryogenic temperature. The main concept here is that the temperature oscillations lead to local freezing/thawing cycles at the freezing front, as the freezing front propagates outwards. Rewcastle et al. (11) have termed this process *dynamic cryosurgery* while Maytal (5) has termed it *cryocycling*. The latter term is adopted for the current study. Rewcastle et al. (11) have presented some preliminary experimental results suggesting that, indeed, cryocycling enhances cryodestruction. However, to the best of the authors' knowledge, verification for these findings has not been reported elsewhere.

One way of performing temperature oscillations at the cryoprobe is by combining an electrical heater with the cryoprobe (9). When using a Joule-Thomson (JT) effect based cryoprobe, another alternative is to switch the working fluid from one having a positive JT coefficient (for example, argon or nitrogen) to one having a negative JT coefficient (one of the quantum gases, i.e. helium, hydrogen, or neon), and consequently changing from cooling to heating (4). Either way, the cryoprobe operation has to be computer-controlled to enable controlled temperature oscillations. The term *high-frequency* is used in this context to distinguish the temperature oscillations of the new application, having a cycling period of less than half a minute, from the traditionally freezing/complete thawing cycles, which have a typical cycling period of 5 to 10 minutes.

---

\* Email: yoed@tx.technion.ac.il; Fax: +972 4 832 4533

The current study provides insight with regard to the thermal effects associated with cryocycling based on numerical simulations. The analysis is given based on the specifications of the only available controlled cryoprobe today which is capable of high-frequency cycling, the Cryo-Hit™ of Galil-Medical, Ltd. Nevertheless, the conclusions of this study are rather general and are not dependent upon a particular hardware.

### Mathematical Modeling

The ordinary heat diffusion equation is assumed to govern the phase change heat transfer process:

$$C \frac{\partial T}{\partial t} = \nabla(k \nabla T) \quad (1)$$

where  $C$  is the specific heat,  $t$  is the time,  $k$  is the thermal conductivity, and  $T$  is the temperature. Assuming biological solutions behave like a NaCl-H<sub>2</sub>O mixture, phase transition is assumed to take place over the temperature range of -22°C and 0°C, where the lower and upper boundaries of phase transition are designated by  $T_s$  and  $T_l$ , respectively. The specific heat and thermal conductivity are assumed to be constant below and above the phase transition temperature range, yielding thermal diffusivity ( $= k/C$ ) of  $1.11 \times 10^{-6}$  and  $1.39 \times 10^{-7}$  m<sup>2</sup>/s, respectively. The thermal conductivity is assumed to vary linearly between the values of 2 W/m-°C at -22°C and 0.5 W/m-°C at 0°C. Following the enthalpy approach within the phase transition temperature range, an effective specific heat is assumed to increase linearly with temperature from a value of 1.8 MJ/m<sup>3</sup>-°C at -22°C to a value of 27 MJ/m<sup>3</sup>-°C at -5°C, and then to decrease linearly to a value of 3.6 MJ/m<sup>3</sup>-°C at 0°C. The integral of the effective specific heat over the phase transition temperature range yields a phase transition enthalpy change of 321.3 MJ/m<sup>3</sup>, which corresponds to a latent heat effect of about 273 MJ/m<sup>3</sup>. The temperature at which the effective specific heat reaches its maximal value, i.e. -5°C, is designated by  $T_m$  and corresponds to the maximal effect of latent heat absorption/release. Further discussion with regard to the enthalpy approach and the effective specific heat of similar problems has been elaborated in (6,10). The numerical technique described above has been validated against experimental data for inanimate materials (7,8), and was applied for parametric estimation of the thermophysical properties of biological tissues in the context of cryosurgery (9).

The blood perfusion effect is neglected in the current analysis for the following reasons: (i) the analysis is focused on the frozen region and on the phase transition region, where no blood perfusion takes place; and, (ii) the heating effect of maximal blood perfusion has been shown to be of a second order in terms of freezing front location and, thus, is not significant for the current analysis (10).

The heat transfer problem is assumed to prevail in a spherically symmetric geometry, with a cryoprobe diameter of 3 mm. It is assumed here that a JT cryoprobe is better modeled in a spherical symmetric geometry, since the heat sink is generated at the cryoprobe tip only, and since the only available cryoprobe capable of controlled cryocycling is JT based. Nevertheless, the effect of cryocycling should not be dependent on a particular coordinate system and, thus, the results are expected to be general.

The heat transfer problem defined above has been solved numerically using the technique suggested in (10) for an infinite domain and a uniform initial temperature distribution,  $T_0$ , of 37°C. An infinite domain from heat transfer considerations is simulated by a finite sphere, which is large enough for the temperature of its outer surface not to be affected by the cooling process at the cryoprobe. It follows that although the outer surface

of the domain has a free boundary condition, its temperature remains unchanged during the simulated period. For the purpose of the current solution, the following cryoprobe cooling protocol is assumed:

$$T(r = R, t) = \begin{cases} T_0 - Ht & t \leq \frac{T_0 - T_{av}}{H} \\ T_{av} - A \sin\left(\frac{2\pi t}{\tau}\right) & t > \frac{T_0 - T_{av}}{H} \end{cases} \quad (2)$$

where  $R$  is the cryoprobe radius,  $H$  is the cooling rate from the initial temperature,  $T_0$ , down to the average cryocycling temperature,  $T_{av}$ ,  $A$  is the cycling amplitude, and  $\tau$  is the cycling period.

### Results and Discussion

Following the specifications provided by Galil-Medical for the Cryo-Hit, two representative cases were studied: (I)  $H=820^\circ\text{C}/\text{min}$ ,  $T_{av} = -120^\circ\text{C}$ ,  $A= 45^\circ\text{C}$ ,  $\tau = 15$  s; and (II)  $H=820^\circ\text{C}/\text{min}$ ,  $T_{av} = -95^\circ\text{C}$ ,  $A= 70^\circ\text{C}$ ,  $\tau = 25$  s. Results of case I are shown in Figs. 1-3. The periodic temperature distributions along one cryocycle of case I, every 1 s interval and after 10 min of simulated cryoprocurement, are shown in Fig. 1. The solid lines represent the cooling stage of the cryocycle, while the dashed lines represent the heating stage. It can be seen that the temperature distribution increases monotonously with the radius, regardless of the cycling stage. As can be expected, temperature gradients are steeper near the cryoprobe in the cooling stage. The effect of thermal inertia can also be seen where temperature distribution curves intersect one another, which results from thermal waves propagation. Similar thermal behavior was found at the short term, at the beginning of cryocycling.

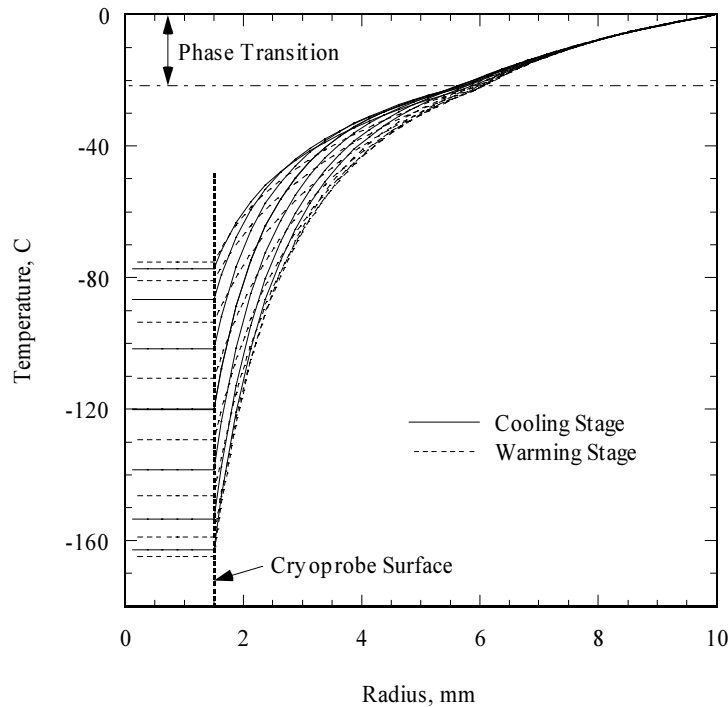


Figure 1: Temperature distribution in case I every 1 s, along a 15 s cryocycle, after 10 min of simulated cryoprocurement.

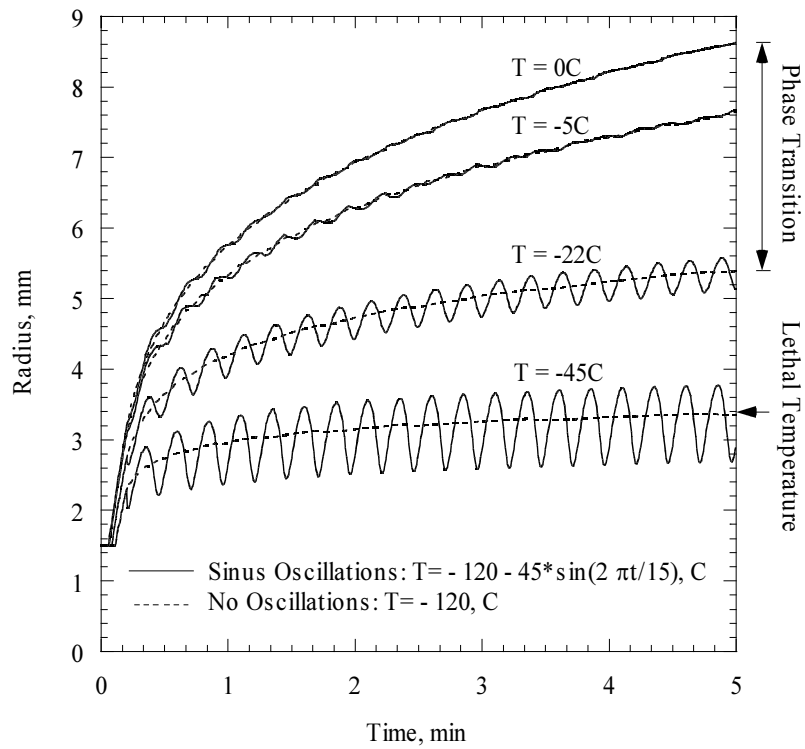


Figure 2: Locations of the isotherms in case I. Solid lines represent a cryocycling procedure, while the dashed lines represent an ordinary procedure with no temperature oscillations.

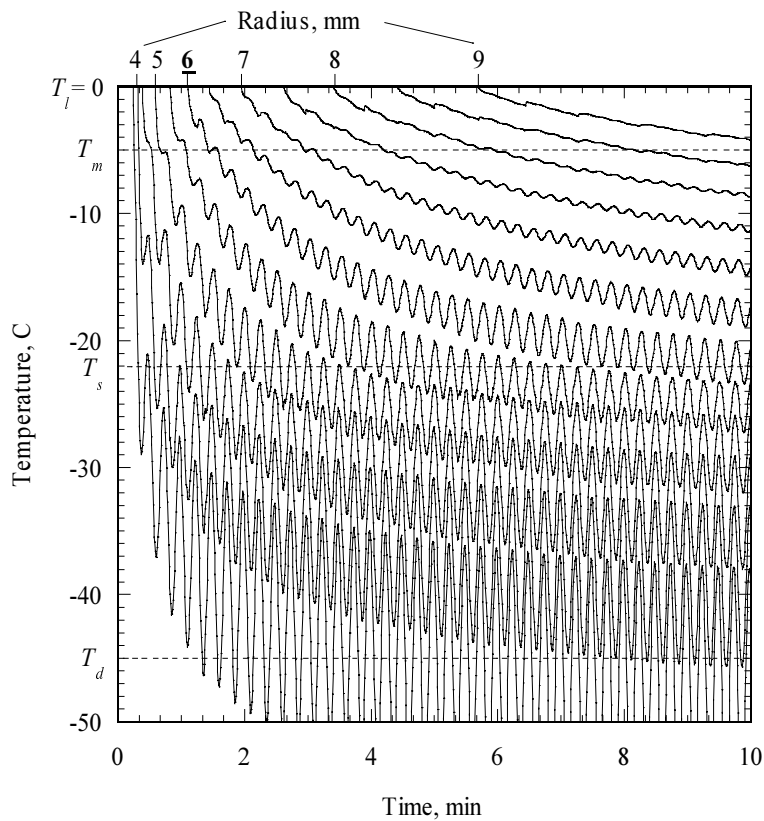


Figure 3: Temperature variation with time at certain specified locations in case I.

The moderating effect of the latent heat on temperature oscillations can further be seen in Fig. 1. The temperature oscillations within the phase transition temperature range are relatively small compared with the forced oscillations at the cryoprobe. Furthermore, the amplitude of oscillations decreases across the phase transition region and is negligible in the unfrozen region. The moderation effect of latent heat appears to be essentially the same, regardless of the phase transition boundaries' location. However, the average thickness of the phase transition region increases as the cryoprocure progresses, a phenomenon which is not related to cryocycling (10).

The locations of the isotherms are shown in Fig. 2, where  $-22^{\circ}\text{C}$  and  $0^{\circ}\text{C}$  define boundaries of the phase transition region, respectively. The isotherm  $-5^{\circ}\text{C}$  defines the location of peak absorption of latent heat and may be regarded as the freezing front. The isotherm  $-45^{\circ}\text{C}$  represents the so-called lethal temperature,  $T_d$ , a threshold below which maximal cell destruction is assumed (2). This isotherm is defined for the purpose of the current thermal analysis only, bypassing the discussion with regard to the actual existence of such a threshold and its value. The solid lines in Fig. 2 represent the locations of the interfaces for an average cycling temperature of  $-120^{\circ}\text{C}$  and an oscillations amplitude of  $45^{\circ}\text{C}$ . Also shown in Fig. 2 are the locations of the isotherms of a similar process but with no cryocycling (by setting the cycling amplitude to  $0^{\circ}\text{C}$ ), represented by the dashed lines.

It can be seen from Fig. 2 that the locations of the isotherms of the problem *with no cryocycling* have almost the average locations of the isotherms of the problem *with cryocycling*. This indicates that a rough approximation for the locations of the isotherms of the mathematical problem of cryocycling can be given by solving a simplified problem dealing solely with the above-mentioned average temperature. Indeed, this conclusion is at no odds with available periodic solutions of heat transfer problems (1). Noting that the average temperature problem is of a first order and the temperature oscillations problem is of a higher order, one can also apply a perturbation technique to generate a cryocycling closed-form solution in a similar manner to the one suggested in (12). However, a closed-form solution can hardly apply to a non-pure material, representing a phase transition temperature range, such as that in the case of biological tissues.

The thickness of the phase transition region is influenced by the cryocycling. For example, the average thickness of this region at one minute is about 1.6 mm (the distance between the isotherms  $-22^{\circ}\text{C}$  and  $0^{\circ}\text{C}$  in Fig. 2). However, the interface of the lower boundary of phase transition moves periodically back and forth, and changes the above thickness in a 0.5 mm interval. Furthermore, the location of the isotherm representing the so-called lethal temperature,  $-45^{\circ}\text{C}$ , oscillates within a 1 mm interval at this point in time.

Figure 3 shows temperature variations with time at certain specific radius locations. It can be seen that the frequency of the temperature oscillations is conserved throughout the frozen region, and that the amplitude of the oscillations decays towards the upper boundary of phase transition. For example, the temperatures at 6 mm radius are discussed (designated by the underlined number at the upper left corner of Fig. 3). The phase transition at this point starts shortly after 1 min from the beginning of the process. The average temperature at this point after 10 min is the lower boundary of phase transition,  $-22^{\circ}\text{C}$ . Within these 9 minutes, the temperature oscillations develop from almost zero to an interval of  $3.5^{\circ}\text{C}$ , while 36 oscillations are counted (one oscillation every 15 s). Note that the number of oscillations within the phase transition temperature range increases with the radius, which results from the decrease in isotherms velocities. On the other hand, the amplitude of oscillations decreases with the radius at any given point in time.

We will now discuss the results of case II, which are shown in Figs. 4-6 below.

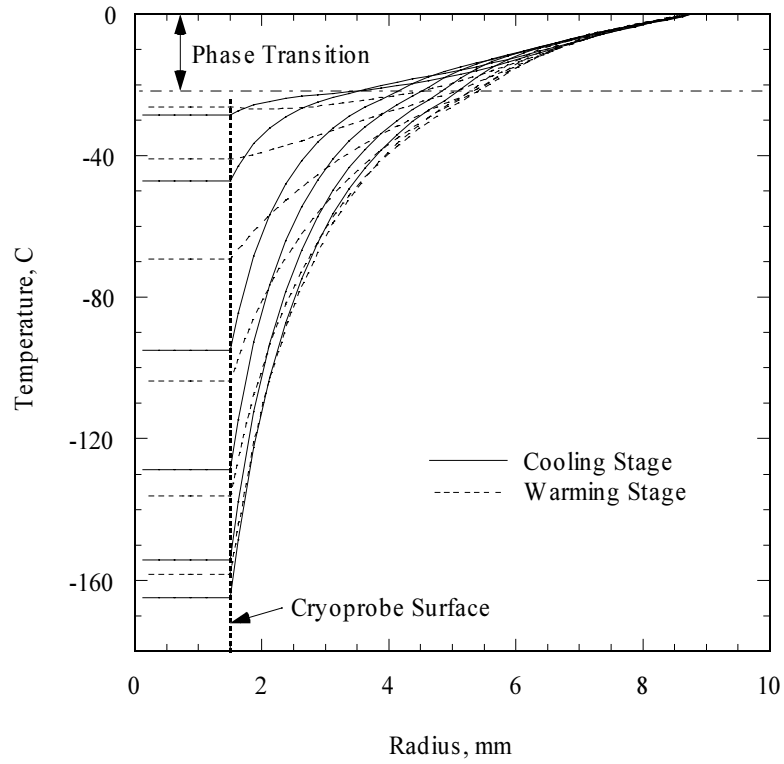


Figure 4: Temperature distribution in case II every 2 s, along a 25 s cryocycle, after 10 min of simulated cryoprotocol.

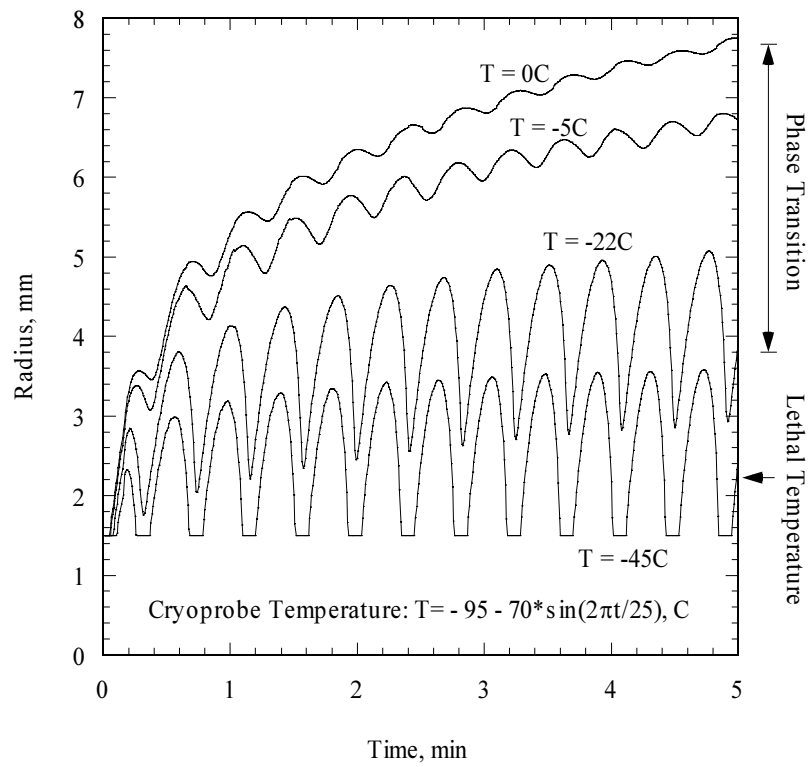


Figure 5: Locations of the isotherms in case II.

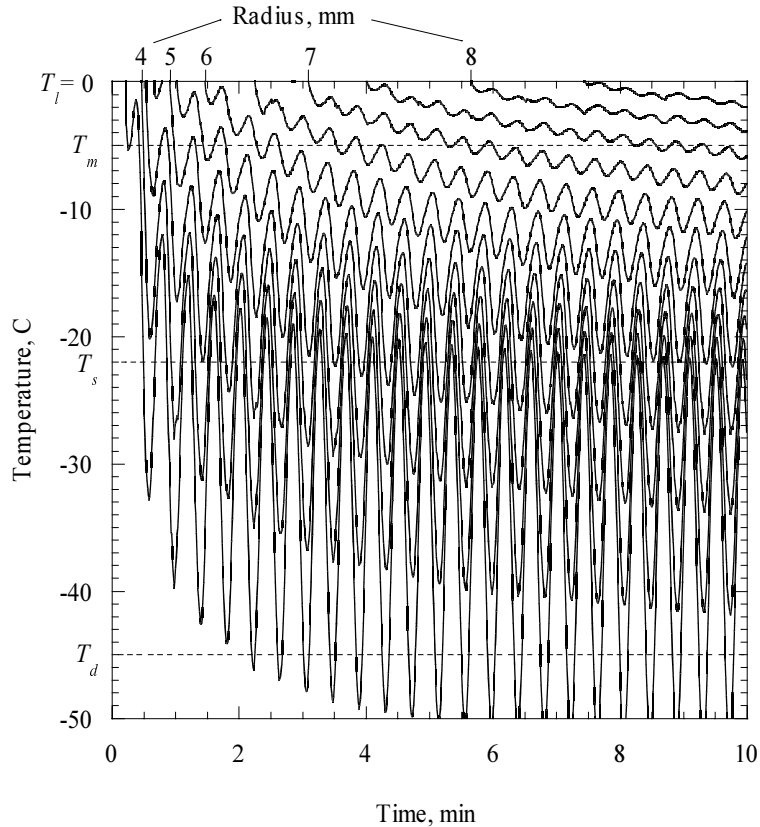


Figure 6: Temperature variation with time at certain specified locations in case II.

Case II differs from case I in the amplitude of oscillations, which is now set to cover the entire cryogenic range of operation, from 3°C below the lower boundary of phase transition and down to the minimal achievable temperature using the Cryo-Hit in cryocycling. As a result, a higher average temperature of -95°C has been chosen for case II. Figure 4 shows similar radial temperature distribution to that shown in Fig. 1 for case I, though amplitudes are larger in case II.

The locations of the isotherms in case II are shown in Fig. 5, where -22°C and 0°C define the phase transition temperature range. Compared to case I, much larger oscillations in the locations of the isotherms are seen in case II, which causes significant periodic changes in the thickness of the phase transition region. For example, the thickness of the phase transition region oscillates at a range of 1.2 and 3.6 mm after about 1 min of operation, and at the range of 2.6 and 4.9 mm after 5 min of operation.

The temperature oscillations within the phase transition region are more noticeable in case II, as can be seen in Fig. 6. For example, the temperature at 6 mm radius after 10 min of operation changes within a 5°C interval, compared to a 3.5°C temperature interval in case I, as is discussed above. Furthermore, the temperature interval around the lower boundary of phase transition is about 12°C after 10 min of operation in case II (but at 5 mm radius).

It is widely accepted that the major effect of cell destruction occurs within the phase transition temperature range due to various regimes of ice formation either extracellularly or intracellularly (2). However, ice formation has been studied in continuous cooling protocol while freezing, and the regime of ice formation due to cryocycling while freezing is difficult to predict. On the one hand, the average temperature variation with time, at any

specific radius, is essentially the same as of the temperature variation in a cryoprocure with no cryocycling. On the other hand, cryocycling introduces much higher instantaneous cooling rates followed by warming rates of the same magnitude during the procedure. At the lower boundary of phase transition for example, the average cooling rate after 10 min is about 0.5°C/min in both cases I and II (at 6 and 5 mm radius, respectively). The instantaneous cooling/warming rates at these locations and at this time vary from +35°C/min to -35°C/min every 7.5 s, and vice versa, in case I; and from +60°C/min to -60°C/min every 12.5 s, and vice versa, in case II. It is possible that a different ice formation regime in this process may explain the observation of higher cell destruction due to cryocycling (11).

Finally, it is emphasized that the reported experimental observations (11) did not result from the highly controlled process suggested here, due to sinusoidal oscillations with a computer controlled apparatus, but rather due to an on-off and manually controlled process.

### Conclusions

Based on the limited experimental observations reported recently and the mathematical analysis present here, it is suggested that the effect of cryocycling on cell survival will be experimentally explored. One line of research can be performed with a temperature programmable cryostage, where periodic temperature oscillations in the various cooling/heating rates and amplitudes shown in Figs. 3 and 6 may simulate different radius locations. Note that the amplitude of temperature oscillations has to increase as the temperature decreases while cooling down through the phase transition temperature range, in order to mimic the cryocycling history on a cryostage. An investigation of ice formation around a cryoprobe during cryocycling can be done in a similar manner to that reported in (3) but with an application of an adequate cryoprobe for cryocycling. The complementary study should deal with *in vivo* studies.

### Acknowledgment

This research has been supported, in part, by Galil-Medical, Ltd. Yoed Rabin acknowledges support of Stanley Imerman Memorial Academic Lectureship - USA. The authors would like to thank Mrs. Miriam Webber for her assistance in preparing this paper.

### References

1. Carslaw, H., and Jaeger, J., *Conduction of Heat in Solids*, Oxford, England, 1956
2. Gage, A., and Baust, J. (1998) *Cryobiology*, **37**(3):171-186
3. Kaprelyants, A.S., et al. (1998) *Cryo-Letters*, **19**(5):303-308
4. Maytal, B-Z. (1996) US patent 5,522,870; 5,577,387
5. Maytal, B-Z. (1997) *Proceedings, The Cryogenic Engineering Conference, Portland, OR*. In press: *Advances in Cryogenic Engineering*, **43**(A):911-918
6. Rabin, Y., et al. (1993) *Int J Heat & Mass Trans*, **36**(3):673-683
7. Rabin, Y., et al. (1995) *Solar Energy*, **55**(6):435-444
8. Rabin, Y., et al. (1996) *Int J Heat & Mass Trans*, **39**(5):1051-1065
9. Rabin, Y., et al. (1996) *Cryobiology*, **33**:82-92
10. Rabin, Y., et al. (1998) *ASME J Biomech Eng*, **120**(1):32-37
11. Rewcastle, J.C., et al. (1998) *Proceedings, Cryo98 – The Annual Meeting of The Society for Cryobiology, Pittsburgh, PA*.
12. Rubinsky, B. (1982) *ASME J Heat Trans*, **104**:196-199